

Origins of the BOLD post-stimulus undershoot

Jean J. Chen^{*}, G. Bruce Pike

McConnell Brain Imaging Centre, Montreal Neurological Institute, McGill University, 3801 University Street, WB325, Montreal, Quebec, H3A 2B4, Canada

ARTICLE INFO

Article history:

Received 21 November 2008

Revised 18 February 2009

Accepted 4 March 2009

Available online 19 March 2009

Keywords:

BOLD post-stimulus undershoot

Cerebral oxygen metabolism

Neurovascular coupling

Cerebral blood flow

Venous cerebral blood volume

fMRI

VERVE

ABSTRACT

The interpretation of the blood-oxygenation level-dependent (BOLD) post-stimulus undershoot has been a topic of considerable interest, as the mechanisms behind this prominent BOLD transient may provide valuable clues on the neurovascular response process and energy supply routes of the brain. Biomechanical theories explain the origin of the BOLD undershoot through the passive ballooning of post-capillary vessels which leads to an increase in venous blood volume (CBV_v, comprising deoxygenated blood in capillary, venular and arteriolar compartments), resulting in susceptibility-induced signal decrease. While there has been substantial evidence supporting a role for venous ballooning, there have also been reports arguing for a prolonged post-stimulus elevation in cerebral oxygenation consumption (CMR_{O₂}) as the primary cause. Furthermore, a contribution of post-stimulus cerebral blood flow (CBF) undershoots has also been demonstrated. To clarify the role of the venous compartment in causing the BOLD undershoot, we performed *in vivo* fMRI measurements of the transient Δ CBV_v, Δ CBF and Δ BOLD responses in healthy humans. We observed a slow post-stimulus return to baseline in venous CBV which supports the existence of a passive “balloon” effect, implying that previous observations of a quicker recovery of the total CBV response may be dominated by arterial CBV change. Our findings also support a significant contribution from the CBF undershoots, which, combined with a slow venous CBV response, would account for much of the BOLD undershoot.

© 2009 Elsevier Inc. All rights reserved.

Introduction

Interpretation of the post-stimulus undershoot in the blood-oxygenation level-dependent (BOLD) signal has been a topic of considerable interest. This BOLD undershoot typically starts between 10 and 20 s after stimulus cessation (Fransson et al., 1999), and is observed for up to 60 s (Bandettini et al., 1997; Mandeville et al., 1999a). This transient feature is present in both the gradient-echo and spin-echo BOLD signal (Jones, 1999; Yacoub et al., 2003). Insignificant inter-subject variation was found in the duration of the undershoot for a given stimulus, but there is significant variation in its magnitude (Mildner et al., 2001). The mechanisms behind this prominent BOLD transient may provide valuable clues on the neurovascular response process and energy supply routes of the brain. In addition, the spatial specificity of the undershoot has been suggested to reflect spatial variability in neuronal activity (Yacoub and Hu, 2001; Yacoub et al., 2006). This discussion, however, is complicated by reports of contradictory observations as to the most likely origin of the undershoot, and there is great interest in reconciling these differences by gaining access to more direct measures of hemodynamics and metabolic processes that govern the BOLD response.

The BOLD post-stimulus undershoot reflects a transient increase in the local deoxy-hemoglobin (dHb) count, which could result from a

number of possible scenarios. Biomechanical models, which attribute the local dHb accumulation to the temporal mismatch between the Δ CBF and venous Δ CBV responses, include the Balloon Model, proposed by Buxton et al. (1998), as well as the Windkessel Model, proposed by Mandeville et al. (1999b). This biomechanical interpretation is supported by a number of human and animal imaging and modeling studies (Friston et al., 2000; Kong et al., 2004; Mandeville et al., 1999a,b, 2001; Nakai et al., 2000; Obata et al., 2004). Notably, using monocrySTALLINE iron-oxide nanocolloid (MION) enhanced CBV imaging (measuring total CBV change) simultaneously with BOLD and laser Doppler flowmetry measurements, Mandeville et al. obtained robust, high signal-to-noise measurements which demonstrated a delayed compliance in CBV in a rat model at 2 T and 4.7 T in response to both focal and global hyperemia (Mandeville et al., 1999a, 2001). Furthermore, there is accumulating evidence that the CBV post-stimulus response is in fact composed of a fast and a slow response, attributed to the elastic arterial recovery from stress and the more passive venous recovery, respectively (Mandeville et al., 1999b; Obrig et al., 1996; Silva et al., 2007).

Alternatively, a transient post-stimulus decoupling between CBF and CMR_{O₂} can also create a post-stimulus accumulation of deoxy-hemoglobin, producing a BOLD undershoot (Frahm et al., 1998; Kruger et al., 1998a,b). In support of this theory, a number of studies have shown evidence of speedy post-stimulus recovery in total CBV, as measured using vascular space occupancy (VASO) as well as contrast-enhanced imaging, which, combined with a fast CBF recovery,

^{*} Corresponding author. Fax: +1 514 398 2975.

E-mail address: jean.chen@mail.mcgill.ca (J.J. Chen).

suggests a post-stimulus CMRO₂ elevation that is decoupled with the hemodynamic response (Frahm et al., 1996, 2008; Krüger et al., 1996; Lu et al., 2004).

In an effort to reconcile these alternate observations, more recent studies (Jin and Kim, 2008; Yacoub et al., 2006; Zhao et al., 2007) have examined the spatial variability of post-stimulus CBF, CBV and BOLD behaviours by imaging at high spatial resolution. Using MION at 9.4 T, Yacoub et al. showed that CBV changes in anesthetized cat cortical tissue persist after stimulus cessation while CBV changes in the surface vessels quickly return to baseline levels, despite a concurrent undershoot in the BOLD signal in both the tissue and surface vessel areas (Yacoub et al., 2006). This was confirmed by later findings from Zhao et al. and Jin et al., who found the most prolonged post-stimulus CBV elevation to be the middle layer, corresponding to the location of the largest BOLD undershoot.

Interestingly, the main debate has not substantially involved another important theory, one that regards the role of CBF. A post-stimulus undershoot in CBF (Behzadi and Liu, 2005; Chen et al., 2007; Chen and Pike, 2008a; Friston et al., 2000; Hoge et al., 1999a; Irikura et al., 1994; Logothetis, 2003; Shmuel et al., 2006; Uludag et al., 2004), which would also result in local dHb accumulation, is a potentially significant contributor. Hoge et al. observed post-stimulus CBF undershoots using human primary visual cortex stimulation at 1.5 T (Hoge et al., 1999a), a finding reproduced by Shmuel et al. in visual stimulation of anesthetized monkeys, and suggested to be associated with a post-stimulus decrease in neuronal activity as revealed in cortical electrophysiological recordings (Shmuel et al., 2006).

Numerous optical studies found the post-stimulus period to be characterized by an undershoot in the concentration of oxy-hemoglobin [Hb] and/or an overshoot in [dHb] (Huppert et al., 2006; Jones et al., 2005; MacIntosh et al., 2003; Schroeter et al., 2006). In particular, using arterial spin labeling (ASL) and BOLD in conjunction with near-infrared spectroscopy (NIRS), an elevation was found in post-stimulus [dHb], mirroring the undershoot in the BOLD and CBF data, with the timing of the post-stimulus elevation in total hemoglobin concentration coinciding with the overshoot in [Hb] (Huppert et al., 2006; MacIntosh et al., 2003). In addition, using optical imaging and laser Doppler flowmetry (LDF) to estimate CBV and CBF changes, respectively, Jones et al. (2001) found delayed post-stimulus [dHb] recovery. However, this was contradicted by an immediate recovery in [Hb] observed by Schroeter et al. (2006). Notwithstanding the abundance of optical data, optical studies are intrinsically limited by penetration depth, spatial resolution and the fundamental differences in the measured parameters compared to MRI. Therefore, the above data, while adding valuable perspective, have not unequivocally resolved the debate.

To the present, there has not been data to address the simultaneous contribution of CBF and venous CBV directly measured in humans. In the context of BOLD contrast, as is addressed in this work, the term “venous blood” refers to all partially deoxygenated blood, specifically, blood from a collective compartment encompassing capillaries and venules, as well as, to a lesser extent, arterioles (Hillman et al., 2007; Hsu and W., 1992). In this study, we sought to clarify these contributions to the BOLD undershoot by performing human fMRI measurements of *in vivo* transient responses in Δ CBV_v, Δ CBF and Δ BOLD evoked by graded visual and sensorimotor stimulation.

Materials and methods

Stimulation paradigm

Sixteen healthy adults (14/2 females/males, ages ranging from 22 to 31 years) participated in the study, and gave informed consent prior to the scanning session. The subjects performed bilateral, sequential finger-to-thumb apposition at low (1.73 Hz) and high (3.46 Hz) frequency (cued by a metronome) while being presented with a radial

yellow/blue checkerboard at low (25%) and high (100%) contrast, reversing contrast at 8 Hz. The low apposition frequency was accompanied by the low contrast checkerboard, the high apposition frequency by the high-contrast checkerboard. The radial checkerboard stimulus was implemented using locally developed software (GLStim) based on the OpenGL graphics library (Silicon Graphics, Mountain View, CA), and was delivered via a back-projection mirror and using a LCD projector with a resolution of 1024 × 768 pixels and a refresh rate of 75 Hz. The visual stimulus occupied between 40° and 45° of the subjects' visual field. The stimulation conditions were alternated with a uniform grey baseline (with luminance level matching that in the presence of the checkerboard). During the resting condition, subjects were requested to look at a white triangular fixation point to maintain attention. Two stimulation-“on” durations were used, namely 24 s and 96 s, each flanked by 16 s and 120 s of pre- and post-stimulus baseline blocks. By varying the stimulation intensity and duration, we expect to modulate the neuronal activity-induced metabolic deficit, thereby providing the conditions to test the theory that the BOLD undershoot is caused mainly by a post-stimulus elevation in CMRO₂, which was suggested to occur mainly to restore this deficit (Lu et al., 2004). Each off/on/off block was repeated twice, and jittered (Yang et al., 2000) to achieve an effective temporal resolution of 2 s. An additional 32 s resting state was inserted at the beginning of the paradigm to permit more robust baseline estimation.

MRI acquisition

All examinations were performed on a Siemens 3 T Magnetom Trio system (Siemens, Erlangen, Germany). Subjects were immobilized using a head holder assembly. An RF body coil was used for transmission and an 8-channel phased array head coil for signal reception. The scanning protocol included a 3D RF-spoiled gradient-echo scan with 1 mm³ isotropic resolution which served as anatomical reference. An 80 s multi-slice BOLD visual and sensorimotor functional scout was acquired to guide slice positioning. During the functional scout, subjects were presented with the high-contrast visual stimulus while performing the high-frequency motor task described in the previous section. Activation *t*-maps were produced using scanner console software, and the coordinates of the regions with the most significant activation in both the visual and sensorimotor regions were used in placing the imaging slice.

The common functional imaging parameters were: FOV/matrix/slice-thickness/TR = 200 × 200 mm²/64 × 64/5 mm/4 s. The fMRI acquisitions were all single-slice, with a voxel size of 3.1 × 3.1 × 5 mm³. The VERVE technique was used to measure changes in venous CBV (Δ CBV_v). Cerebral-spinal fluid (CSF) suppression was performed at an inversion time of 1100 ms for a repetition time of 4 s. This was followed by the VERVE magnetization preparation, composed of a pair of non-selective 90° tip-down and tip-up pulses flanking an MLEV phase-cycled CPMG train made up of non-selective composite 90°_x–180°_y–90°_x refocusing pulses for either fast or slow refocusing. The corresponding τ_{180}^F and τ_{180}^S were 3 ms and 24 ms, respectively, forming a refocusing train with duration of 192 ms; this duration, combined with the echo-spacing of 6.8 ms for the TSE readout resulted in an effective VERVE echo time (TE) of 198.8 ms. One cycle of phase-chopping was used in the slice-selective excitation pulse. Venous blood oxygenation, which is necessary for VERVE calibration, was obtained for each subject *in vivo* based on internal jugular oximetry using a magnetization-prepared segmented EPI sequence (Foltz et al., 1999), cardiac-gated using a finger oxymeter.

CBF and BOLD data were simultaneously acquired using pulsed ASL, which was previously shown to provide BOLD measurements equivalent to those acquired with standard BOLD (Chen and Parrish, 2007). The QUIPSS II ASL technique (Wong et al., 1997) was used, with ASSIST background suppression (Ye et al., 2000). The protocol contained the following parameters: TI₁/TI₂/TE/labeling thickness/

gap = 700 ms/1300 ms/25 ms/100 mm/5 mm. Two asymmetric BASSI pre-saturation pulses (Warnking and Pike, 2004, 2006) in the imaging region were followed by an adiabatic BASSI inversion pulse in the labeling region (gap of 5 mm). EPI readout (bandwidth = 2170 Hz/pixel) was used.

Data processing

Motion correction of the CBF, CBV_v and BOLD datasets was performed across all runs using AFNI's *2dimreg* software (Cox, 1996). The frames with estimated translation exceeding 1 mm or rotation greater than 1° were excluded from the analysis. The CBF and CBV_v data were then aligned to each other using MincTools (Montreal Neurological Institute, Canada), such that all functional data were mutually aligned. The functional data were spatially smoothed using a two-dimensional Gaussian filter with a full-width at half-maximum (FWHM) of 6 mm. Drift was removed by subtracting from each voxel's time course the low-frequency components of its discrete cosine transform, with a cutoff frequency at half of the stimulation paradigm frequency.

The difference between the slow- and the fast-refocused images was calculated, and a calibration factor computed from the venous oxygenation was used to convert $\Delta VERVE$ to ΔCBV_v on a per-subject basis (Stefanovic and Pike, 2005). As customary, ΔCBF was calculated from the difference between the control and tag ASL images, while $\Delta BOLD$ was obtained as the average between tag and control. Finally, sinc interpolation was performed to correct the timing differences between the control and tag images in the CBF and BOLD data, as well as between the fast- and slow-refocused images in the VERVE data. This also permitted the correction of potential BOLD contamination in ASL data due to this timing difference (Lu et al., 2006).

We used *fMRIstat* (Worsley et al., 2002) to identify areas of statistically significant task correlation based on the generalized linear model, with corrections for multiple comparisons. The gamma-variate hemodynamic response function, which has been found to provide robust activation correlation for all modalities, was used for the analysis. The BOLD, CBF and CBV_v ROIs were defined for each subject by thresholding the t -maps (at the t -value corresponding to a significance level of $p < 0.05$ after correction for multiple comparisons). Visual and sensorimotor cortex ROIs were differentiated based on anatomical considerations, with sensorimotor ROIs constrained to the banks of the Rolandic fissure, and the visual ROI in close proximity to the calcarine sulcus. The time course analysis was based on the overlap between the significantly activated voxels in the CBF, CBV_v and BOLD t -maps obtained from the functional run with the highest activation t values. Theoretically, ASL is more sensitive to arterioles and capillaries (Wong et al., 1997), whereas VERVE is more sensitive to intravascular changes in the capillaries and the post-capillary compartment (i.e. venules and veins), and BOLD is sensitive to both intra- and extra-vascular contributions, stemming from oxygenation changes in capillaries, venules and veins. Therefore, although each

voxel is likely to contain all compartments, it is likely that restricting the ROI to those activated in the CBV_v , CBF and BOLD t -maps would reduce emphasis of the arterial and venous macrovasculature. In addition, the use of the overlapping ROIs targets the interaction of CBF and CBV_v in the exactly the same location as the corresponding BOLD undershoot. Finally, to minimize overall bias towards the highest t -scores, the CBF- CBV_v -BOLD overlapped ROI from the functional run with the most robust activation (the highest t -scores) was applied to all other functional runs.

The CBF, CBV_v and BOLD time courses derived from each ROI were temporally low-pass-filtered (Hanning filter, FWHM = 6 s). Piecewise fitting of the time courses to a double-gamma hemodynamic response function (Glover, 1999) was performed using the unconstrained nonlinear least-square method, i.e. the onset and offset transient portions of the time courses were fit separately, such that neither is biased by the temporal features of the other. The time-to-fall (T_f) of the time courses (the time taken to fall to the half-maximum) was estimated from the modeled time courses, as illustrated in Fig. 3. The statistically significant undershoots (at the $p < 0.05$ level) were identified, and their durations quantified via their respective full-width at half-maximum ($FWHM_{US}$). Both T_f and $FWHM_{US}$ were corrected for the low-pass filter FWHM. Finally, the normalized post-stimulus response amplitude (A_{PS}) for each time course was calculated as the measured post-stimulus response amplitude within the BOLD $FWHM_{US}$ time frame divided by the corresponding positive response amplitude. Thus, A_{PS} enabled us to assess the behaviours of all measurements precisely when the BOLD post-stimulus undershoot occurs. The dependence of T_f , $FWHM_{US}$ and A_{PS} on stimulus type, stimulation intensity and the stimulation-“on” duration was assessed using 3-way ANOVA, while inter-modality differences were evaluated using Student's t -test. Finally, the correlation between undershoot parameters in matching sets of time courses was assessed using linear regression.

Results and discussion

Results

CBV_v , CBF and BOLD t -maps for one subject under high-intensity visual and sensorimotor stimulation are shown in Fig. 1 for 96 s stimulus-“on” duration, overlaid with the corresponding anatomical reference image. VERVE- CBV_v , ASL-CBF and BOLD have distinct sensitivities and specificities, as can be seen from the peaks in the t -maps. Although each voxel is likely to contain multiple vascular compartments, it is likely that using the overlap between all three sets of t -maps would increase the probability of including voxels with high capillary and venular weighting.

The group-averages of the measured time courses for ΔCBV_v , ΔCBF and BOLD are shown in Fig. 2 for the 96 s stimulation condition in the visual and sensorimotor regions. The post-stimulus dynamics can be clearly seen in these measured time courses, particularly the slow

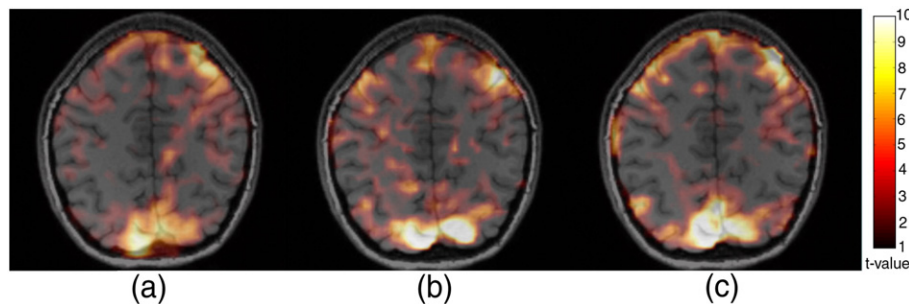


Fig. 1. Sample CBV_v (a), CBF (b) and BOLD (c) activation t -maps from one subject during 100% contrast visual stimulus accompanied by 3.46 Hz bilateral finger tapping. Only voxels presenting significant activation in all three maps were used in the time course analysis.

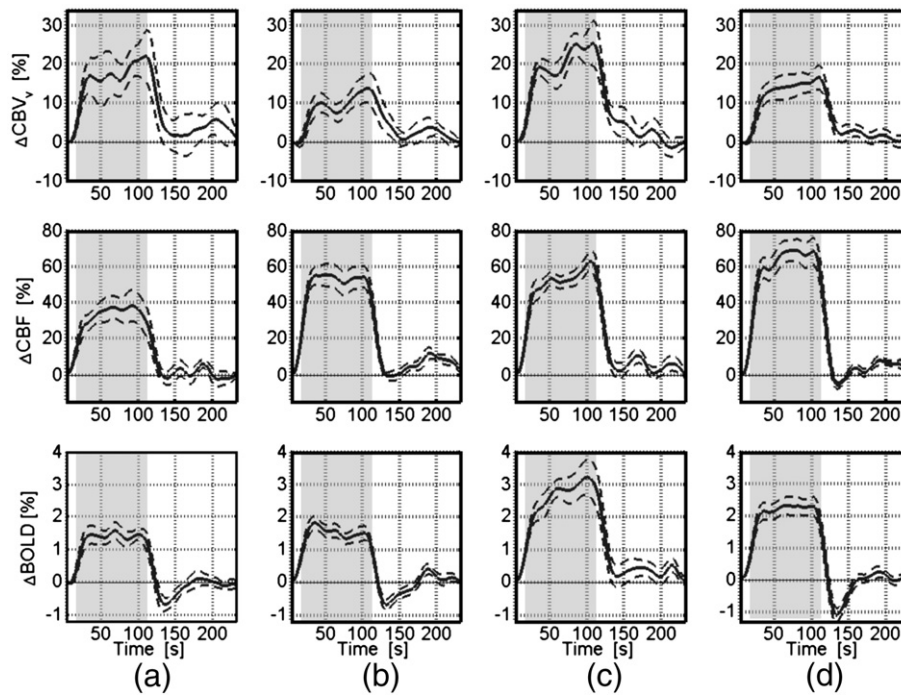


Fig. 2. Group-averages of measured time courses for 96 s stimulation duration: (a) low-intensity sensorimotor stimulation ($n = 11$); (b) low-intensity visual stimulation ($n = 13$); (c) high-intensity sensorimotor stimulation ($n = 12$); (d) high-intensity visual stimulation ($n = 14$). The dashed lines indicate the standard error, and the stimulation-on period is indicated by the shaded region. In order to enable better visualization of the general transient dynamics, these time courses were smoothed using a low-pass Hanning filter with a 13 s FWHM.

recovery of ΔCBV_v , as well as the well-defined undershoots in the visual ΔCBF and all BOLD responses. However, to enable the quantitative assessment of these features, modeling was performed on these time courses. The positive response amplitude is defined as the average time course amplitude above the FWHM of the positive response, and is therefore unbiased by stimulation duration. The post-stimulus response amplitude was normalized by the positive response amplitude to compare the transient responses between data acquired using different modalities.

A sample set of the measured CBV_v , CBF and BOLD time courses obtained under visual stimulation is shown in blue in Fig. 3, for short (Figs. 3a, c, e) and long (Figs. 3b, d, f) stimulation duration, along with their least-square fits to the double-gamma-variate model. As shown in Fig. 3g, all transient parameters were normalized to enable cross-modality and cross-subject comparison and categorization.

All transient parameter estimates were categorized as shown in Fig. 4, and assessed for their dependence on stimulation intensity, duration and type. The rate of post-stimulus recovery was judged based on T_f , while the undershoot size was assessed based on FWHM_{US} and A_{PS} . The BOLD recovery rate and undershoot size were found to be independent of stimulation intensity (Fig. 4a) and duration (Fig. 4b). However, the BOLD A_{PS} and FWHM_{US} were both significantly influenced by the type of stimulation (i.e. visual vs. sensorimotor), with $p = 0.01$ for both cases (Fig. 4c). The CBF undershoot was also independent of stimulation intensity and duration, but as in the BOLD case, both A_{PS} and FWHM_{US} were significantly different between the visual and sensorimotor cases ($p = 0.01$ and 0.03 , respectively), as shown in Fig. 4c. Lastly, no dependence on stimulation intensity, duration or type was observed in any of the CBV_v transient parameters.

The transient parameters were compared according to data type (i.e. BOLD, CBF or CBV_v). As significant differences were found between the transient responses to visual and sensorimotor stimulation, the data were further divided according to the stimulation type, shown in Fig. 5. The first main observation is that T_f for CBV_v (visual: 16.4 ± 2.6 s, sensorimotor: 19.1 ± 3.4 s) was longer than either that of

CBF (visual: 5.0 ± 0.3 s, sensorimotor: 10.0 ± 1.2 s) or BOLD (visual: 5.4 ± 1.8 s, sensorimotor: 8.3 ± 1.2 s). The CBF and BOLD T_f were statistically indistinguishable. This was the case for both visual ($p < 0.01$) and sensorimotor stimulation ($p < 0.05$). The BOLD response exhibited more prominent and consistent undershoot features than both CBF and CBV_v , with the longest FWHM_{US} in all categories and the largest A_{PS} . This was also common to both visual ($p < 0.001$ for both FWHM_{US} and A_{PS}) and sensorimotor stimulation ($p < 0.05$ for FWHM_{US} and A_{PS}). Another notable observation is that undershoots were consistently observed in the visual CBF responses, reflected by the negative average CBF response (Fig. 5a). In the sensorimotor case, the CBF response did not show significant undershooting, and the average CBF A_{PS} was statistically indistinguishable from zero, reflecting an early return of CBF to baseline (Fig. 5b). However, under both groupings, the average A_{PS} for CBV_v was consistently above zero, characteristic of an elevated venous CBV over the course of the BOLD undershoots.

Discussion

In this study, we sought to shed light on the possible mechanisms underlying the BOLD post-stimulus undershoot by directly measuring venous CBV changes, as well as ΔCBF and BOLD, in healthy human subjects during graded visual and sensorimotor stimulation of varying durations. At 3 T, the VERVE technique provided robust measures (Chen and Pike, 2008b) which are in agreement with contrast-enhanced measurements of venous volume change in animals (Lee et al., 2001). The CBF and BOLD response amplitudes to graded stimulation were in excellent agreement with the literature (Hoge et al., 1999a; Ito et al., 2001; Kastrup et al., 2002). Both the positive BOLD CBF responses increased with stimulation intensity (Fig. 2). However, this was not the case for CBV_v , likely because the CBF– CBV_v relationship is characterized by a shallow trend, with CBF variations far exceeding those in CBV_v (Chen and Pike, 2008b; Lee et al., 2001). Our focus is, nonetheless, on the physiological and biomechanical mechanism underlying the transient response. We have developed a

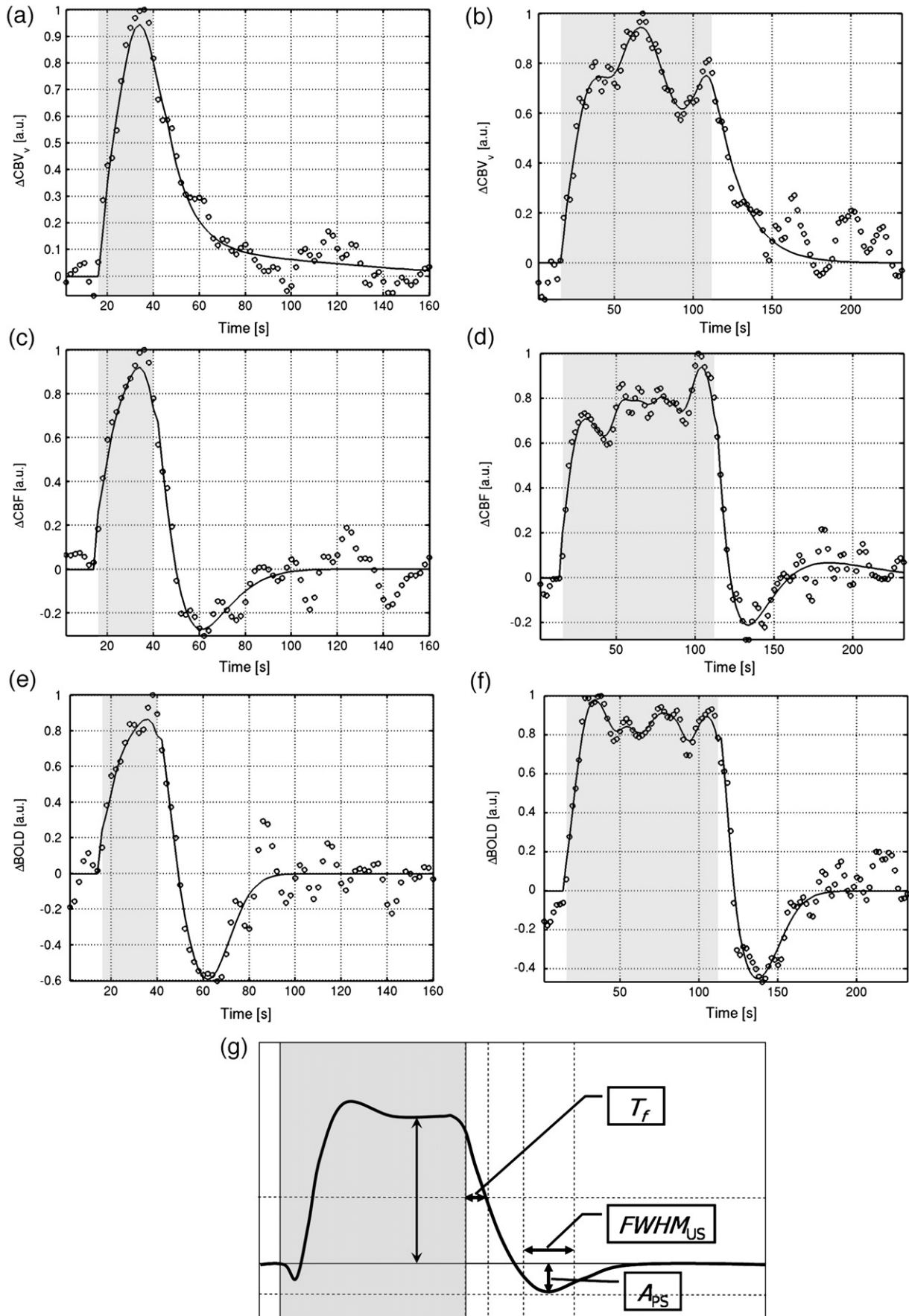


Fig. 3. Sample measured (open dots) and fitted (solid line) CBV_v (a, b), CBF (c, d) and $BOLD$ (e, f) time courses (normalized), for the high-intensity visual stimulation in one subject. The transient parameters measured from the modeled time courses are illustrated in (g).

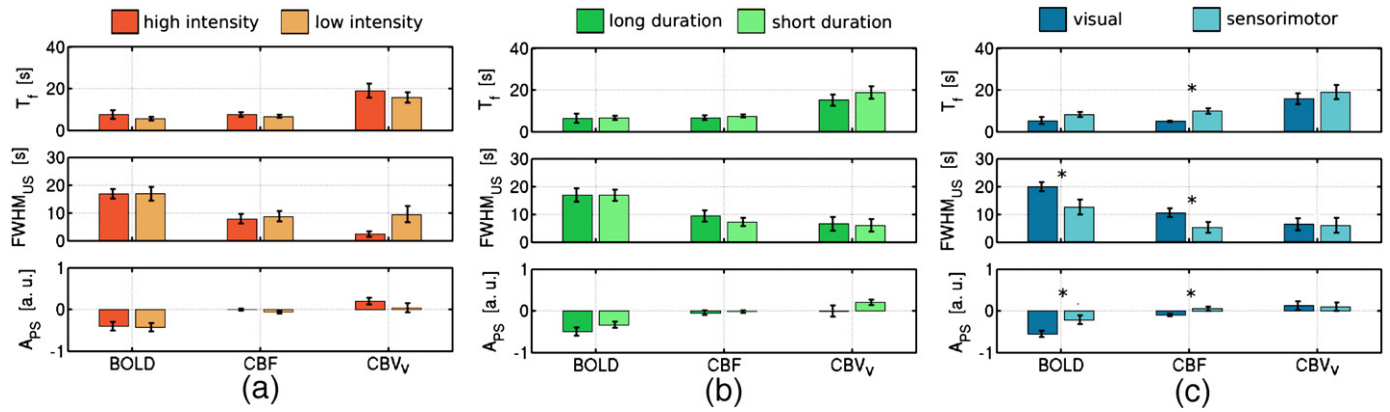


Fig. 4. The group-average post-stimulus transient parameters, time-to-fall (T_f), normalized post-stimulus response amplitude (A_{PS}) and undershoot full-width-half-maximum ($FWHM_{US}$) are shown for CBV_v , CBF and BOLD responses, classified by stimulus intensity (a), duration (b) and type (c). Only the CBF and BOLD data showed statistically significant undershoots, with CBV_v being characterized by the longest T_f . No stimulation intensity or duration dependence was found in any of the parameters (a, b), but both the BOLD and CBF undershoots (A_{PS} and $FWHM_{US}$) were significantly larger in the visual than the sensorimotor case. In addition, the CBF T_f were both significantly longer in the visual than the sensorimotor region. Asterisks indicate significant difference ($p < 0.05$).

set of measures, namely the time-to-fall (T_f), the normalized post-stimulus response (A_{PS}) and the FWHM of the post-stimulus undershoots ($FWHM_{US}$), which characterize multi-modal post-stimulus transient response without being biased by the vastly different response amplitudes.

CBF post-stimulus undershoot

The first important finding of this study is that the CBF response, as measured using QUIPSS II ASL, exhibited post-stimulus undershoots, the amplitude of which was correlated with the BOLD undershoot amplitude. The use of surround subtraction (Lu et al., 2006) minimized the potential of the CBF transients being biased by oxygenation effects, and hence precluded the possibility of the CBF undershoots being solely the result of BOLD contamination. CBF undershoots have been observed in both MRI and optical imaging literature (Hoge et al., 1999a,b; Huppert et al., 2006; Shmuel et al., 2006; Uludag et al., 2004). However, a number of studies reported the absence of CBF undershoots under stimulation conditions similar to those studied here and using similar analysis techniques (Kruger et al., 1998b; Lu et al., 2004). While the exact origin of this difference is

unclear, it has been suggested that the precise type of stimulus or paradigm influence the occurrence of the CBF transients (Hoge et al., 1999a). Although the positive CBF change has been found to be independent of the stimulus type, delayed and stimulus-dependent finer-scaled flow adjustments (Kruger et al., 1998b) may contribute to diverging post-stimulus responses.

The CBF undershoot has been suggested to be the result of an autoregulatory CBF feedback mechanism of neuronal origin (Friston et al., 2000; Uludag et al., 2004). Using cortical electrophysiological recordings, Shmuel et al. demonstrated post-stimulus undershoots in neuronal activity following visual stimulation, providing further support for a neuronal origin to the CBF undershoot (Devor et al., 2007; Hamel, 2006; Shmuel et al., 2006; Zonta et al., 2003), which is also in concordance with predictions based on the “arteriolar compliance model”, in which neural activity modulates the compliance of arteriolar smooth muscle, and hence the initiation of the CBF response (Behzadi and Liu, 2005). In our study, the dependence of the CBF post-stimulus response (in terms of T_f , $FWHM_{US}$ and A_{PS}) on stimulation type may be a reflection of the differences in the neuronal activities elicited by visual and sensorimotor activation. However, we

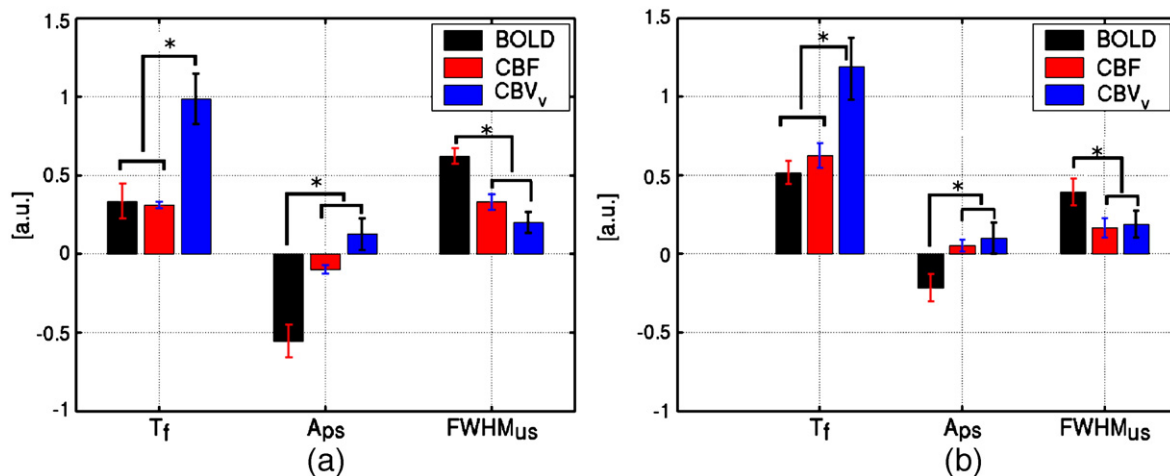


Fig. 5. All post-stimulus transient parameters were summarized under the visual (a) and sensorimotor (b) categories. T_f , A_{PS} and $FWHM_{US}$ were rescaled differently for better ensemble visualization. The CBV_v data was characterized by a T_f that was significantly longer than that of either CBF or BOLD for both visual ($p < 0.01$) and sensorimotor stimulation ($p < 0.05$), as well as post-stimulus elevation. The CBF and BOLD T_f were mutually indistinguishable. Furthermore, the BOLD response exhibited more prominent and consistent undershoot features than both CBF and CBV_v , with the longest $FWHM_{US}$ in all categories and the most negative A_{PS} . This was also common to both visual ($p < 0.001$ for both $FWHM_{US}$ and A_{PS}) and sensorimotor stimulation ($p < 0.05$ for both $FWHM_{US}$ and A_{PS}). The CBF and CBV_v undershoot sizes did not differ significantly. Asterisks indicate significant difference ($p < 0.05$).

do not preclude regional variability in vascular structure and hemodynamic response, which could have also contributed to the visual-sensorimotor CBF response difference.

Venous compliance

Another important finding of this study is that the CBV_v post-stimulus responses were clearly characterized by a slower return to baseline relative to either CBF or BOLD. This observation is thus in support of a passive and lagging dilatatory component to the CBV response as described by Buxton et al. (1998) and observed by Mandeville et al. (1999a,b). However, in this case, the definition of “venous blood” encompasses all deoxygenated vascular compartments, and our measurement of ΔCBV_v is a weighted average of the CBV response in all these vascular compartments, expected to include capillaries and venules (Hillman et al., 2007; Hutchison et al., 2006), and to a lesser extent, arterioles and veins. The nature of the venous blood volume response was also reflected by previous observations of a passive dilatatory component of CBV decrease (Mandeville et al., 1998; Shen et al., 2008). Furthermore, as the ΔCBV_v transient parameters were uninfluenced by the intensity, duration or type of the stimulation, our findings support a primarily biomechanical response in venous blood volume to neuronal activation, hence a response modulated largely by changes in blood flow.

CBV_v manifested significantly longer T_f than both CBF and BOLD, as was also observed in previous fMRI studies (Leite et al., 2002; Mandeville et al., 1999a). Having reduced the contribution of draining veins from the analysis (by using the CBF– CBV_v –BOLD t -map overlap), our findings likely reflect primarily venular response, and support biomechanical theories regarding the contribution of the venous CBV to the BOLD undershoot (Aubert and Costalat, 2002; Buxton et al., 1998; Mandeville et al., 1999b). Furthermore, in Mandeville’s modified Windkessel Model, the temporal evolution of total CBV was described as a rapid elastic response of the postarteriolar compartment, approximately synchronized with the CBF response, followed by slow venous relaxation of stress (Mandeville et al., 1999b), the latter being the chief cause of the BOLD undershoot. This bi-phasic CBV behaviour was experimentally confirmed by Silva et al. (2007) and Shen et al. (2008). The close agreement between our CBV_v T_f measurements and the characteristics of the slow component (Mandeville et al., 1999b) is evidence that the fast component is likely more arterially weighted. Indeed, this was postulated by the arteriolar compliance model, in which baseline vascular state affects the dynamic response by changing the relative contributions of the active smooth muscle component and the passive connective tissue component to the overall vessel compliance. When coupled with the passive Balloon Model, the arterial compliance model was able to predict the observed CBF and BOLD response at various baseline conditions (Behzadi and Liu, 2005).

Our findings of delayed venous compliance are in agreement with optical imaging spectroscopy studies (Hoge et al., 2005; Malonek et al., 1997; Martindale et al., 2003). Malonek et al. noted an increase in [dHb] accompanied by a simultaneous increase in total hemoglobin concentration [tHb], presumably reflecting an early total blood volume increase. Their observation of a CBF change lagging [tHb] changes by 1 to 2 s supports the notion of active neurovascular regulation of blood volume in the capillary bed and the existence of a delayed, passive process of capillary filling (Malonek et al., 1997). A post-stimulus elevation in [tHb] and overshoot in [dHb] was also observed by Hoge et al. using diffuse optical tomography (Hoge et al., 2005), in line with a prolonged CBV recovery observed by Martindale et al. (2003). The relative timings of these parameters were found to be consistent between the sensorimotor and the visual systems (Boden et al., 2007), in line with our observations.

The current results differ from findings of a more instantaneous CBV recovery observed in studies measuring total ΔCBV using the vascular space occupancy (VASO) and gadolinium-enhanced bolus

tracking techniques (Frahm et al., 2008; Lu et al., 2004; Yang et al., 2004). Notably, VASO measured a CBV response that decreased earlier than BOLD or CBF, but lagged behind that of BOLD by 5 to 10 s in its eventual return to baseline (Lu et al., 2003, 2004). This is in contrast with our finding of a slower initial CBV_v drop-off relative to BOLD and CBF. Also in contrast with these earlier findings, our data show that venous CBV remains elevated over the whole duration of the BOLD undershoot, as indicated by positive $CBV_v A_{PS}$, and is likely to play a role in inducing the BOLD undershoot. These observations likely reflect dynamic differences between venous and total CBV change.

As described earlier, total ΔCBV transitions, involving both the arterial and venous compartments, have on several occasions been found to be biphasic. Venous blood volume change has been shown to contribute to only 40% to total ΔCBV (Lee et al., 2001), implying that arterial dilation is likely to contribute most to total percent CBV change, as was reported by various groups (Lee et al., 2001; Okazawa et al., 2001; Zhao et al., 2007). Thus, arterial CBV is expected to contribute substantially to the “fast” phase of total CBV response described above, and total ΔCBV , being the weighted average of its arterial and venous components, is likely to exhibit a faster initial post-stimulus recovery reflective of CBF recovery. As we observed a decidedly slower post-stimulus response in CBV_v , we can attribute the slow component in total CBV change to primarily capillary and venular contribution, as was observed in recent cortical two-photon microscopy studies (Hillman et al., 2007; Hutchison et al., 2006).

Variations in the spatial specificity of the CBV measurements could also result in different observation of the CBV transient. Using MION imaging at high spatial resolution, Yacoub et al. showed that the post-stimulus CBV response was distinctly slower in the deeper parenchyma than near the cortical surface (Yacoub et al., 2006). Their findings are consistent with a CBV response with primarily capillary and venular weighting, and are in remarkable agreement with our observations, derived from ROIs with high microvascular weighting. As the BOLD signal is modulated by partially deoxygenated volume instead of total CBV, the quantification of CBV contributions to the BOLD undershoot should be based primarily upon CBV_v measurements. The fractional CBV changes associated with neuronal activation are expected to be weighted more towards deeper cortical layers, while the BOLD response is generally greater in the draining pial veins on the cortical surface, as reflected by the spatial profile analysis in previous works (Shen et al., 2008; Zhao et al., 2007). Nonetheless, given the spatial resolution employed in most *in vivo* human fMRI studies, including the current study, it is not possible to spatially resolve the various vascular compartments or cortical layers reliably. Thus, the BOLD and CBV_v responses observed in this study are both weighted averages of the contributions from capillaries, venules and veins (pial and intra-cortical) across multiple cortical layers.

BOLD post-stimulus response

BOLD showed significant and pronounced undershoots, as expected. The BOLD A_{PS} estimates were significantly larger than those of CBF in all cases ($p < 0.05$), showing that the undershoot figures most prominently in the BOLD time course. The BOLD undershoot amplitude did not vary significantly with the positive ΔCBF , in agreement with previous observations (Hoge et al., 1999a).

Significant correlation was found between the BOLD and CBF A_{PS} , strengthening support for the existence of a non-negligible CBF contribution to the BOLD undershoot. In addition, the BOLD undershoot amplitude was significantly larger in the visual region, in agreement with recent studies (Buckner et al., 1998; Chiarelli et al., 2007). The same was true for $FWHM_{US}$, and both the undershoot amplitude and duration dependency coincide with findings with the CBF transients, while no such dependency was observed with CBV_v . Given that the CBF response is likely to have a significant neuronal correlation (Hamel, 2006; Hyder et al., 1998), which is likely to vary with stimulus type, this visual-sensorimotor difference in the BOLD

undershoot not only adds support for a strong contribution of the CBF undershoot to the BOLD undershoot, but further implicates the role of a neuronal contribution in producing the BOLD undershoots. However, the BOLD T_f was not significantly different between the visual and sensorimotor categories, while that of CBF was (Fig. 4c). This observation may be attributed to the concurrent and significant CBV_v contribution, as the $CBV_v T_f$ was also found to be independent of stimulus type. This finding further indicates that neuronally mediated factors such as CBF and biomechanical factors such as CBV_v both contribute to the formation of the BOLD undershoots, though in different fashions.

Differences in visual and sensorimotor neuronal activity are likely to result from fundamental differences in the stimuli, as well as from the neural and glial heterogeneity that characterizes the cerebral cortex (Jezzard et al., 2003). The cortex is also characterized by heterogeneity in vascular density (Cavaglia et al., 2001). It was found that surface layers of the cortex (layers I to III), which are associated with the highest level of vascularization, are also the locations of the largest BOLD changes and undershoots (Shen et al., 2008; Silva et al., 2007). In addition, the occipital lobe surface is more vascularized than the surface of the sensorimotor areas (Duvernoy et al., 1981). These facts may also attribute the BOLD undershoot difference between visual and sensorimotor stimulation to the regionally specific capillary density. However, given that no significant distinction was made between the visual and sensorimotor transient CBV_v responses hints that this regional difference in hemodynamics is not solely the result of local vascular construct, but may have a neuronal contributor that is determined by the nature of the stimuli themselves. Indeed, Hoge et al. extensively studied the visual stimulus-dependence in the BOLD and CBF dynamic responses, and found that certain visual patterns, such as the polychromatic radial checkerboard used in this study, produced more robust and pronounced BOLD undershoots than others (Hoge et al., 1999a; Kruger et al., 1998b). Further along this theme, Fox et al. studied the BOLD transients across a wider variety of tasks, and reported that while the occurrence of undershoot is brain region-dependent, the amplitudes of the undershoots depends on the type of task, and hence on the underlying neuronal activity (Fox et al., 2005). It is therefore reasonable to postulate that the BOLD undershoot also stems from stimulation-specific metabolic triggers, which are likely to be reflected in the corresponding CBF response. Boden et al. found that changes in [Hb] lead those in [dHb] in the sensorimotor system but not in the visual system, an effect shown to result from a systemic response accompanying sensorimotor activity, but otherwise found no fundamental physiological difference between cortical hemodynamic regulation in motor and visual cortex (Boden et al., 2007). This systemic response was explored earlier by Vafaee and Gjedde, who attributed the difference mainly to a difference in attention requirements (Vafaee and Gjedde, 2004). Unlike during visual stimulation, where the subject's attention is required both during activation and baseline, the sensorimotor system is required to be at rest between stimulation blocks. This motor task paradigm is likely to emphasize the subjects' level of anticipation, hence elevating baseline CBF in spite of the subjects being at rest. The ensuing elevation in baseline oxygenation may give rise to a smaller BOLD undershoot. The BOLD post-stimulus undershoot is strongly influenced by baseline hemodynamic and metabolic conditions. Cohen et al. observed that the post-stimulus undershoot resolved more quickly with hypocapnia and appeared to be abolished with hypercapnia (Cohen et al., 2002), a behaviour that was reproduced by Behzadi et al. using the arterial compliance model (Behzadi and Liu, 2005). This was further confirmed by Lindauer et al., who observed no undershoot during hyperoxia, and more pronounced undershoots during hypoxia (Lindauer et al., 2003).

The existence of a non-hemodynamic basis for the undershoot was supported by simulations by Jones (1999), giving occasion to theories

in which metabolic factors are the sole origin (Frahm et al., 2008; Lu et al., 2004). It has been postulated that the BOLD undershoot is incurred by elevated post-stimulus oxygen metabolism ($CMRO_2$), which is needed to restore the ion gradients depleted by action potential generation (Lu et al., 2004). Derived from measurements of total ΔCBV , this $CMRO_2$ elevation was further suggested to occur in the absence of prolonged CBF or CBV_v elevation, resulting in a transient dissociation between $CMRO_2$ and CBF. Notwithstanding the obviously slower response in post-stimulus ΔCBV_v , which is one of our main arguments in favour of a biomechanical contribution, as well as the potential caveats of inferring CBV dynamics from a plasma-based technique, our analysis of the BOLD undershoot sensitivities also argue against a post-stimulus $\Delta CMRO_2$ elevation being the main cause of the BOLD undershoot. Evidently, the level of oxygen consumption, which modulates dHb content, would depend on the type of stimulus and the level of activation elicited, as the latter contributes directly to the degree of depletion experienced in the ion gradients, and hence the level of metabolic deficit. Thus, should the sustained $CMRO_2$ (the existence of which was to eliminate this deficit) be the only cause of the BOLD undershoot, the amplitude and duration of the latter would be expected to correlate with the intensity and/or duration of the stimulus. However, in this study, neither the BOLD post-stimulus undershoot amplitude nor duration was influenced by stimulation duration or intensity over the range studied by the above authors. This echoes our previous finding of BOLD undershoot independence on stimulus duration over a wider range (Chen et al., 2007). It is therefore evident that sustained metabolism cannot be the sole cause of the BOLD undershoots.

Finally, certain animal studies have reported small BOLD undershoots (Silva et al., 2007) during motor stimulation while others show the contrary (Huttunen et al., 2007; Mandeville et al., 1999a). However, the necessity of using anesthetic agents in these studies could have substantially modified functional and hemodynamic transients. Urethane has been known to reduce baseline CBF (Osborne, 1997) and halve the rate of action potentials (Simons et al., 1992), while isoflurane has been shown to increase baseline perfusion and prolong activation due to its inhibitive effect on potassium channels (Kuroda et al., 2000). Huttunen et al. found that urethane-anesthetized rodents exhibited BOLD responses over a much wider range of stimulus frequencies than alpha-chloralose-anesthetized rats, which only responded to low-frequency stimuli. Although tight neural-hemodynamic coupling was observed in both cases (Huttunen et al., 2007), the varying baseline conditions are expected to seriously influence the BOLD undershoot, and as described earlier, baseline CBF elevation undermines BOLD undershoots. Furthermore, Palmer et al. reported fluctuations in partial carbon dioxide pressure and pH in alpha-chloralose anesthetized rats (Palmer et al., 1999). These parameters can affect the hemodynamic response to neuronal activation and could conceivably lead to variation in one or more aspects of the response within and between animals as physiological condition changes over time.

We have shown clear evidence for the contribution of prolonged venous CBV_v elevation to the BOLD post-stimulus undershoot, as proposed by the Balloon and Windkessel models. However, this biomechanical factor is likely not the only contributor to the undershoot, the occurrence of which is dependent on the stimulus (Hoge et al., 1999a) and baseline (Fox et al., 2005). The BOLD undershoot has previously been suggested to result solely from ongoing metabolism and flow-metabolism uncoupling (Frahm et al., 2008; Lu et al., 2004), and was supported by a faster post-stimulus drop-off in total ΔCBV . However, such observations may reflect a predominance of arterial CBV in their measurements, which is not the main modulator of the BOLD signal. Our results also support CBF undershoots as a significant contributor to the BOLD post-stimulus undershoot, whether engendered through biomechanical or neuronal means.

Acknowledgments

This research was supported by the Natural Sciences and Engineering Research Council of Canada (J. J. C.) and the Canadian Institutes of Health Research (G. B. P.).

References

- Aubert, A., Costalat, R., 2002. A model of the coupling between brain electrical activity, metabolism, and hemodynamics: application to the interpretation of functional neuroimaging. *NeuroImage* 17, 1162–1181.
- Bandettini, P.A., Kwong, K.K., Davis, T.L., Tootell, R.B., Wong, E.C., Fox, P.T., Belliveau, J.W., Weisskoff, R.M., Rosen, B.R., 1997. Characterization of cerebral blood oxygenation and flow changes during prolonged brain activation. *Hum. Brain Mapp.* 5, 93–109.
- Behzadi, Y., Liu, T.T., 2005. An arteriolar compliance model of the cerebral blood flow response to neural stimulus. *NeuroImage* 25, 1100–1111.
- Boden, S., Obrig, H., Köhncke, C., Benav, H., Koch, S.P., Steinbrink, J., 2007. The oxygenation response to functional stimulation: is there a physiological meaning to the lag between parameters? *NeuroImage* 36, 100–107.
- Buckner, R.L., Goodman, J., Burock, M., Rotte, M., Koutstaal, W., Schacter, D., Rosen, B., Dale, A.M., 1998. Functional-anatomic correlates of object priming in humans revealed by rapid presentation event-related fMRI. *Neuron* 20, 285–296.
- Buxton, R.B., Wong, E.C., Frank, L.R., 1998. Dynamics of blood flow and oxygenation changes during brain activation: the balloon model. *Magn. Reson. Med.* 39, 855–864.
- Cavaglia, M., Dombrowski, S.M., Drazba, J., Vasanji, A., Bokesch, P.M., Janigro, D., 2001. Regional variation in brain capillary density and vascular response to ischemia. *Brain Res.* 910, 81–93.
- Chen, J.J., Pike, G.B., 2008a. Measuring hemodynamic contributions to the BOLD post-stimulus undershoot. Proceedings of the 14th International Meeting of the Organization for Human Brain Mapping, Melbourne. p. 656.
- Chen, J.J., Pike, G.B., 2008b. Steady-state relationship between cerebral blood flow and venous blood volume. Proceedings of the 16th Meeting of the ISMRM, Toronto. p. 1909.
- Chen, Y., Parrish, T., 2007. Is ASL-BOLD equivalent to standard BOLD? 13th Annual Meeting of the Organization for Human Brain Mapping, Chicago. p. 265.
- Chen, J.J., Advani, K., Pike, G.B., 2007. Analysis of the biomechanical origin of the BOLD post-stimulus undershoot. Proceedings of the 13th International Meeting of the Organization for Human Brain Mapping, Chicago. p. 47.
- Chiarelli, P.A., Bulte, D., Gallician, D., Piechnik, S.K., Wise, R., Jezzard, P., 2007. Flow-metabolism coupling in human visual, motor and supplementary motor areas assessed by magnetic resonance imaging. *Magn. Reson. Med.* 57, 538–547.
- Cohen, E.R., Ugurbil, K., Kim, S.G., 2002. Effect of basal conditions on the magnitude and dynamics of the blood oxygenation level-dependent fMRI response. *J. Cereb. Blood Flow Metab.* 22, 1042–1053.
- Cox, R.W., 1996. AFNI: software for analysis and visualization of functional magnetic resonance neuroimages. *Comput. Biomed. Res.* 29, 162–173.
- Devor, A., Tian, P., Nishimura, N., Teng, I.C., Hillman, E.M.C., Narayanan, S.N., Ulbert, I., Boas, D.A., Kleinfeld, D., Dale, A.M., 2007. Suppressed neuronal activity and concurrent arteriolar vasoconstriction may explain negative blood oxygenation level-dependent signal. *J. Neurosci.* 27, 4452–4459.
- Duvernoy, H.M., Delon, S., Vannson, J.L., 1981. Cortical blood vessels of the human brain. *Brain Res. Bull.* 7, 519–579.
- Foltz, W.D., Merchant, N., Downar, E., Stainsby, J.A., Wright, G.A., 1999. Coronary venous oximetry using MRI. *Magn. Reson. Med.* 42, 837–848.
- Fox, M.D., Snyder, A.Z., Barch, D.M., Gusnard, D.A., Raichle, M.E., 2005. Transient BOLD responses at block transitions. *NeuroImage* 28, 956–966.
- Frahm, J., Kruger, G., Merboldt, K.D., Kleinschmidt, A., 1996. Dynamic uncoupling and recoupling of perfusion and oxidative metabolism during focal brain activation in man. *Magn. Reson. Med.* 35, 143–148.
- Frahm, J., Kruger, G., Merboldt, K.-D., Kleinschmidt, A., 1998. Dynamic uncoupling and recoupling of perfusion and oxidative metabolism during focal brain activation in man. *Magn. Reson. Med.* 35, 143–148.
- Frahm, J., Baudewig, J., Kallenberg, K., Kastrup, A., Merboldt, K.D., Dechent, P., 2008. The post-stimulation undershoot in BOLD fMRI of human brain is not caused by elevated cerebral blood volume. *NeuroImage* 40, 473–481.
- Fransson, P., Gunnar Kruger, K.-D.M., Frahm, J., 1999. MRI of functional deactivation: temporal and spatial characteristics of oxygenation-sensitive responses in human visual cortex. *NeuroImage* 9, 611–618.
- Friston, K.J., Mechelli, A., Turner, R., Price, C.J., 2000. Nonlinear responses in fMRI: the balloon model, volterra kernels, and other hemodynamics. *NeuroImage* 12, 466–477.
- Glover, G.H., 1999. Deconvolution of impulse response in event-related BOLD fMRI. *NeuroImage* 9, 416–429.
- Hamel, E., 2006. Perivascular nerves and the regulation of cerebrovascular tone. *J. Appl. Physiol.* 100, 1059–1064.
- Hillman, E.M.C., Devor, A., Bouchard, M.B., Dunn, A.K., Krauss, G.W., Skoch, J., Bacskai, B.J., Dale, A.M., Boas, D.A., 2007. Depth-resolved optical imaging and microscopy of vascular compartment dynamics during somatosensory stimulation. *NeuroImage* 35, 89–104.
- Hoge, R.D., Atkinson, J., Gill, B., Crelier, G.R., Marrett, S., Pike, G.B., 1999a. Stimulus-dependent BOLD and perfusion dynamics in human V1. *NeuroImage* 9, 573–585.
- Hoge, R.D., Atkinson, J., Gill, B., Crelier, G.R., Marrett, S., Pike, G.B., 1999b. Young Investigator's Award: Investigation of BOLD signal dependence on cerebral blood flow and oxygen consumption: the deoxyhemoglobin dilution model. *Magn. Reson. Med.* 42, 849–863.
- Hoge, R.D., Franceschini, M.A., Covolan, R.J.M., Huppert, T., Mandeville, J.B., Boas, D.A., 2005. Simultaneous recording of task-induced changes in blood oxygenation, volume, and flow using diffuse optical imaging and arterial spin-labeling MRI. *NeuroImage* 25, 701–707.
- Hsu, R., W., S.T., 1992. Analysis of oxygen exchange between arterioles and surrounding capillary-perfused tissue. *J. Biomech. Eng.* 114, 227–232.
- Huppert, T.J., Hoge, R.D., Diamond, S.G., Franceschini, M.A., Boas, D.A., 2006. A temporal comparison of BOLD, ASL, and NIRS hemodynamic responses to motor stimuli in adult humans. *NeuroImage* 29, 368–382.
- Hutchison, E.B., Stefanovic, B., Koretsky, A.P., Silva, A.C., 2006. Spatial flow-volume dissociation of the cerebral microcirculatory response to mild hypercapnia. *NeuroImage* 32, 520–530.
- Huttunen, J.K., Gröhn, O., Penttonen, M., 2007. Coupling between simultaneously recorded BOLD response and neuronal activity in the rat somatosensory cortex. *NeuroImage* 39, 775–785.
- Hyder, F., Shulman, R.G., Rothman, D.L., 1998. A model for the regulation of cerebral oxygen delivery. *J. Appl. Physiol.* 85, 554–564.
- Irikura, K., Maynard, K.I., Moskowitz, M.A., 1994. Importance of nitric oxide synthase inhibition to the attenuated vascular responses induced by topical L-nitroarginine during vibrissal stimulation. *J. Cereb. Blood Flow Metab.* 14, 45–48.
- Ito, H., Takahashi, K., Hatazawa, J., Kim, S.G., Kanno, I., 2001. Changes in human regional cerebral blood flow and cerebral blood volume during visual stimulation measured by positron emission tomography. *J. Cereb. Blood Flow Metab.* 21, 608–612.
- Jezzard, P., Matthews, P.M., Smith, S.M., 2003. Functional MRI: An Introduction to Methods. Oxford University Press, USA, Oxford.
- Jin, T., Kim, S.G., 2008. Cortical layer-dependent dynamic blood oxygenation, cerebral blood flow and cerebral blood volume responses during visual stimulation. *NeuroImage* 43, 1–9.
- Jones, M., Berwick, J., Johnston, D., Mayhew, J., 2001. Concurrent optical imaging spectroscopy and laser-Doppler flowmetry: the relationship between blood flow, oxygenation, and volume in rodent barrel cortex. *NeuroImage* 13, 1002–1015.
- Jones, M., Berwick, J., Hewson-Stoate, N., Gias, C., Mayhew, J., 2005. The effect of hypercapnia on the neural and hemodynamic responses to somatosensory stimulation. *NeuroImage* 27, 609–623.
- Jones, R.A., 1999. Origin of the signal undershoot in BOLD studies of the visual cortex. *NMR Biomed.* 12, 299–308.
- Kastrup, A., Kruger, G., Neumann-Haefelin, T., Glover, G.H., Moseley, M.E., 2002. Changes of cerebral blood flow, oxygenation, and oxidative metabolism during graded motor activation. *NeuroImage* 15, 74–82.
- Kong, Y., Zheng, Y., Johnston, D., Martindale, J., Jones, M., Billings, S., Mayhew, J., 2004. A model of the dynamic relationship between blood flow and volume changes during brain activation. *J. Cereb. Blood Flow Metab.* 24, 1382–1392.
- Krüger, G., Kleinschmidt, A., Frahm, J., 1996. Dynamic MRI sensitized to cerebral blood oxygenation and flow during sustained activation of human visual cortex. *Magn. Reson. Med.* 35, 797–800.
- Krüger, G., Kleinschmidt, A., Frahm, J., 1998a. Dynamic MRI sensitized to cerebral blood oxygenation and flow during sustained activation of human visual cortex. *Magn. Reson. Med.* 35, 797–800.
- Krüger, G., Kleinschmidt, A., Frahm, J., 1998b. Stimulus dependence of oxygenation-sensitive MRI responses to sustained visual activation. *NMR Biomed.* 11, 75–79.
- Kuroda, Y., Murakami, M., Tsuruta, J., Murakawa, T., Shiroyama, Y., 2000. Effects of sevoflurane and isoflurane on the ratio of cerebral blood flow/metabolic rate for oxygen in neurosurgery. *J. Anesth.* 14, 124–128.
- Lee, S.P., Duong, T.Q., Yang, G., Iadecola, C., Kim, S.G., 2001. Relative changes of cerebral arterial and venous blood volumes during increased cerebral blood flow: implications for BOLD fMRI. *Magn. Reson. Med.* 45, 791–800.
- Leite, F.P., Tsao, D., Vanduffel, W., Fize, D., Sasaki, Y., Wald, L.L., Dale, A.M., Kwong, K.K., Orban, G.A., Rosen, B.R., Tootell, R.B., Mandeville, J.B., 2002. Repeated fMRI using iron oxide contrast agent in awake, behaving macaques at 3 Tesla. *NeuroImage* 16, 283–294.
- Lindauer, U., Gethmann, J., Kuhl, M., Kohl-Bares, M., Dirnagl, U., 2003. Neuronal activity-induced changes of local cerebral microvascular blood oxygenation in the rat: effect of systemic hyperoxia or hypoxia. *Brain Res.* 975, 135–140.
- Logothetis, N.K., 2003. The underpinnings of the BOLD functional magnetic resonance imaging signal. *J. Neurosci.* 23, 3963–3971.
- Lu, H., Golay, X., Pekar, J.J., van Zijl, P.C.M., 2003. Functional magnetic resonance imaging based on changes in vascular space occupancy. *Magn. Reson. Med.* 50, 263–274.
- Lu, H., Golay, X., Pekar, J.J., van Zijl, P.C.M., 2004. Sustained poststimulus elevation in cerebral oxygen utilization after vascular recovery. *J. Cereb. Blood Flow Metab.* 24, 764–770.
- Lu, H., Donahue, M.J., van Zijl, P.C.M., 2006. Detrimental effects of BOLD signal in arterial spin labeling fMRI at high field strength. *Magn. Reson. Med.* 56, 546–552.
- MacIntosh, B.J., Klassen, L.M., Menon, R.S., 2003. Transient hemodynamics during a breath hold challenge in a two part functional imaging study with simultaneous near-infrared spectroscopy in adult humans. *NeuroImage* 20, 1246–1252.
- Malonek, D., Dirnagl, U., Lindauer, U., Yamada, K., Kanno, I., Grinvald, A., 1997. Vascular imprints of neuronal activity: relationships between the dynamics of cortical blood flow, oxygenation, and volume changes following sensory stimulation. *Proc. Natl. Acad. Sci. U. S. A.* 94, 14826–14831.
- Mandeville, J.B., Marota, J.J.A., Ayata, C., Moskowitz, M.A., Weisskoff, R.M., Rosen, B.R., 1999a. MRI measurement of the temporal evolution of relative CMRO₂ during rat forepaw stimulation. *Magn. Reson. Med.* 42, 944–951.
- Mandeville, J.B., Marota, J.J.A., Ayata, C., Zaharchuk, G., Moskowitz, M.A., Rosen, B.R., Weisskoff, R.M., 1999b. Evidence for a cerebral postarteriole windkessel with delayed compliance. *J. Cereb. Blood Flow Metab.* 19, 679–689.
- Mandeville, J.B., Marota, J.J.A., Kosofsky, B.E., Keltner, J.R., Weissleder, R., Rosen, B.R., Weisskoff, R.M., 1998. Dynamic functional imaging of relative cerebral blood volume during rat forepaw stimulation. *Magn. Reson. Med.* 39, 615–624.

- Mandeville, J.B., Jenkins, B.G., Kosofsky, B.E., Moskowitz, M.A., Rosen, B.R., Marota, J.J., 2001. Regional sensitivity and coupling of BOLD and CBV changes during stimulation of rat brain. *Magn. Reson. Med.* 45, 443–447.
- Martindale, J., Mayhew, J., Berwick, J., Jones, M., Martin, C., Johnston, D., Redgrave, P., Zheng, Y., 2003. The hemodynamic impulse response to a single neural event. *J. Cereb. Blood Flow Metab.* 23, 546–555.
- Mildner, T., Norris, D.G., Schwarzbauer, C., Wiggins, C.J., 2001. A qualitative test of the balloon model for BOLD-based MR signal changes at 3 T. *Magn. Reson. Med.* 46, 891–899.
- Nakai, T., Matsuo, K., Kato, C., Tekehara, Y., Isoda, H., Moriya, T., Okada, T., Sakahara, H., 2000. Post-stimulus response in hemodynamics observed by functional magnetic resonance imaging—difference between the primary sensorimotor area and the supplementary motor area. *Magn. Reson. Imaging* 18, 1215–1219.
- Obata, T., Liu, T.T., Miller, K.L., Luh, W.M., Wong, E.C., Frank, L.R., Buxton, R.B., 2004. Discrepancies between BOLD and flow dynamics in primary and supplementary motor areas: application of the balloon model to the interpretation of BOLD transients. *NeuroImage* 21, 144–153.
- Obrig, H., Hirth, C., Junge-Hulsing, J.G., Doge, C., Wolf, T., Dirnagl, U., Villringer, A., 1996. Cerebral oxygenation changes in response to motor stimulation. *J. Appl. Physiol.* 81, 1174–1183.
- Okazawa, H., Yamauchi, H., Sugimoto, K., Toyoda, H., Kishibe, Y., Takahashi, M., 2001. Effects of acetazolamide on cerebral blood flow, blood volume, and oxygen metabolism: a positron emission tomography study with healthy volunteers. *J. Cereb. Blood Flow Metab.* 21, 1472–1479.
- Osborne, P.G., 1997. Hippocampal and striatal blood flow during behavior in rats: chronic laser Doppler flowmetry study. *Physiol. Behav.* 61, 485–492.
- Palmer, J., de Crespigny, A., Williams, S., Busch, E., van Bruggen, N., 1999. High-resolution mapping of discrete representational areas in rat somatosensory cortex using blood volume-dependent functional MRI. *NeuroImage* 9, 383–392.
- Schroeter, M.L., Kupka, T., Mildner, T., Uludag, K., Cramona, D.Y.v., 2006. Investigating the post-stimulus undershoot of the BOLD signal—a simultaneous fMRI and fNIRS study. *NeuroImage* 30, 349–358.
- Shen, Q., Ren, H., Duong, T.Q., 2008. CBF, BOLD, CBV, and CMRO2 fMRI signal temporal dynamics at 500-msec resolution. *J. Magn. Reson. Imaging* 27, 599–606.
- Shmuel, A., Augath, M., Oeltermann, A., Logothetis, N.K., 2006. Negative functional MRI response correlates with decreases in neuronal activity in monkey visual area V1. *Nat. Neurosci.* 9, 569–577.
- Silva, A.C., Koretsky, A.P., Duyn, J.H., 2007. Functional MRI impulse response for BOLD and CBV contrast in rat somatosensory cortex. *Magn. Reson. Med.* 57, 1110–1118.
- Simons, D.J., Carvell, G.E., Hershey, A.E., Bryant, D.P., 1992. Responses of barrel cortex neurons in awake rats and effects of urethane anesthesia. *Exp. Brain Res.* 91, 259–272.
- Stefanovic, B., Pike, G.B., 2005. Venous refocusing for volume estimation: VERVE functional magnetic resonance imaging. *Magn. Reson. Med.* 53, 339–347.
- Uludag, K., Dubowitz, D.J., Yoder, E.J., Restom, K., Liu, T.T., Buxton, R.B., 2004. Coupling of cerebral blood flow and oxygen consumption during physiological activation and deactivation measured with fMRI. *NeuroImage* 23, 148–155.
- Vafaei, M.S., Gjedde, A., 2004. Spatially dissociated flow-metabolism coupling in brain activation. *NeuroImage* 21, 507–515.
- Warnking, J.M., Pike, G.B., 2004. Bandwidth-modulated adiabatic RF pulses for uniform selective saturation and inversion. *Magn. Reson. Med.* 52, 1190–1199.
- Warnking, J.M., Pike, G.B., 2006. Reducing contamination while closing the gap: BASSI RF pulses in PASL. *Magn. Reson. Med.* 55, 865–873.
- Wong, E.C., Buxton, R.B., Frank, L.R., 1997. Implementation of quantitative perfusion imaging techniques for functional brain mapping using pulsed arterial spin labeling. *NMR Biomed.* 10, 237–249.
- Worsley, K.J., Liao, C.H., Aston, J., Petre, V., Duncan, G.H., Morales, F., Evans, A.C., 2002. A general statistical analysis for fMRI data. *NeuroImage* 15, 1–15.
- Yacoub, E., Hu, X., 2001. Detection of the early decrease in fMRI signal in the motor area. *Magn. Reson. Med.* 45, 184–190.
- Yacoub, E., Duong, T.Q., van De Moortele, P.F., Lindquist, M., Adriany, G., Kim, S.G., Ugurbil, K., Hu, X., 2003. Spin-echo fMRI in humans using high spatial resolutions and high magnetic fields. *Magn. Reson. Med.* 49, 655–664.
- Yacoub, E., Ugurbil, K., Harel, N., 2006. The spatial dependence of the poststimulus undershoot as revealed by high-resolution BOLD- and CBV-weighted fMRI. *J. Cereb. Blood Flow Metab.* 26, 634–644.
- Yang, Y., Engelen, W., Pan, H., Xu, S., Silbersweig, D.A., Stern, E., 2000. A CBF-based event-related brain activation paradigm: characterization of impulse-response function and comparison to BOLD. *NeuroImage* 12, 287–297.
- Yang, Y., Gu, H., Stein, E.A., 2004. Simultaneous MRI acquisition of blood volume, blood flow, and blood oxygenation information during brain activation. *Magn. Reson. Med.* 52, 1407–1417.
- Ye, F.Q., Frank, J.A., Weinberger, D.R., McLaughlin, A.C., 2000. Noise reduction in 3D perfusion imaging by attenuating the static signal in arterial spin tagging (ASSIST). *Magn. Reson. Med.* 44, 92–100.
- Zhao, F., Jin, T., Wang, P., Kim, S.-G., 2007. Improved spatial localization of post-stimulus BOLD undershoot relative to positive BOLD. *NeuroImage* 34, 1084–1092.
- Zonta, M., Angulo, M.C., Gobbo, S., Rosengarten, B., Hossmann, K.A., Pozzan, T., Carmignoto, G., 2003. Neuron-to-astrocyte signaling is central to the dynamic control of brain microcirculation. *Nat. Neurosci.* 6, 43–50.